

Huarui Zhang, Xiaoxia Tang, Qing Pan, Lei Zhou, Chungeng Zhou and Hu Zhang\*

# Microstructure and Mechanical Property Optimization of NiTiAl-based Alloys: Directional Solidification in Novel Ceramic Crucibles

**Abstract:** Directional solidification technique was successfully used to prepare highly reactive NiTiAl-based alloys using novel  $Y_2O_3$ -coated crucibles. Compared with the as-cast alloys fabricated by vacuum arc melting, the microstructure of the directionally solidified alloys was optimized and mechanical properties remarkably improved. After directional solidification, the microstructure of the alloys became much finer and preferentially grew along [001] orientation. The tensile strength and strain of the directionally solidified alloys at 1550°C were promoted to 1240 MPa and 2.1% respectively, which were 91.4% and 75% higher than that of the as-cast alloys. The strength increased up to 1328 MPa and 1419 MPa after homogenizing treating. The  $Y_2O_3$ -coated crucibles assured significant purification effect of the alloys. The maximum oxygen increase in the steady-state region of the ingot obtained at 1750°C was no more than 0.014 wt. %.

**Keywords:** NiTiAl-based alloy, microstructure, mechanical property, crucible, directional solidification

---

\*Corresponding author: **Hu Zhang:** School of Materials Science and Engineering, Beihang University, Beijing 100191, China  
E-mail: zhanghu@buaa.edu.cn

**Huarui Zhang, Xiaoxia Tang, Qing Pan, Lei Zhou, Chungeng Zhou:** School of Materials Science and Engineering, Beihang University, Beijing 100191, China

---

## 1 Introduction

Because of their excellent shape memory effect and superelasticity, NiTi alloys have been successfully used in various fields, such as home appliances, medical and electronic devices [1, 2]. Since Koizumi et al. [3] reported that Al addition into NiTi alloys substituting for Ti atoms could remarkably enhance the compression strength of the near-equiatomic NiTi alloys at room and elevated temperatures, NiTiAl-based alloys as novel potential high

temperature structural materials for aerospace applications have attracted much attention.

To date, nearly all the NiTiAl-based alloy ingots are prepared by vacuum arc melting (VAM) or vacuum induction melting (VIM) [3–5]. However, these processes generally result in microstructure heterogeneity and unavoidable metallurgical defects, such as shrinkage cavity and porosity [6]. In contrast with the above methods, directional solidification (DS) technique can not only control precise microstructure but also eliminate metallurgical defects, which are beneficial to the mechanical properties [7, 8]. However, limited efforts have been made to investigate NiTiAl-based alloys by DS technology.

Based on previous study, it is well known that the Bridgman-type liquid-metal-cooled (LMC) directional solidification with ultra high-temperature and high vacuum condition in ceramic crucibles is attractive for achieving sufficient superheating temperature, great chemical and microstructure homogeneity and complex geometry [9]. However, when the highly reactive alloys are melted in oxide ceramic crucibles, the oxygen contamination seems inevitable and even produces oxide inclusions in the alloys due to the metal-crucible reactions although the process was performed under ultra-high vacuum condition [10]. The contamination will deteriorate the microstructure and mechanical properties of the alloys [9]. Therefore, in order to obtain desired alloy microstructure with high purification effect and improve the mechanical properties, developing suitable crucibles for high quality DS highly reactive alloys is challenging. Among the common oxides,  $Y_2O_3$  exhibits the most thermodynamic stability [11]. Taking into account the thermal shock resistance and high cost of the  $Y_2O_3$ ,  $Y_2O_3$ -coated crucible is expected to be a suitable crucible for high quality DS NiTiAl-based alloys.

The aim of this work is to optimize the microstructure and improve the mechanical properties of the novel NiTiAl-based alloys by LMC DS technique with high temperature and vacuum. The microstructure evolution and the tensile properties of the alloys were discussed. As the crucibles played an important role in the quality of the ingots, the effect of crucible materials on the

purification, microstructure and properties of the alloys was also discussed.

## 2 Experimental

With nominal compositions of Ni-44Ti-5Al-2Nb-1Mo (at.%), the master alloys were produced using commercial titanium sponge (99.76 wt.%), Ni block (99.98%), Al ingot (99.99%), Nb sheet (99.98%), and Mo (99.90%) as raw materials which were carefully cleaned with an acetone solution in an ultrasonic bath before being dried at 150°C for 120 min. A 1.1 kg homogeneous master alloy button containing 0.024 wt.% oxygen was prepared by 5 repeated cycles of vacuum arc melting in high purity protecting argon. It was cut, prior to DS, into several alloy bars with a diameter of about 14 mm by a wire-electro discharge machining (WEDM) technique, and were polished, cleaned and dried. For comparison, newly-designed  $Y_2O_3$  (purity 99.9 wt.%, mean grain size 3  $\mu\text{m}$ ) coated  $Al_2O_3$  (double layered  $Y_2O_3/Al_2O_3$ ) crucibles [12] and conventional single layered  $Al_2O_3$  crucibles (purity 99.5 wt.%, mean grain size 10  $\mu\text{m}$ ) with dimensions of 20 mm o.d.  $\times$  15 mm i.d.  $\times$  200 mm length were used respectively. The average thickness of the  $Y_2O_3$  coating in the former was about 0.6 mm (see Ref 12 for more details about it).

DS was carried out in a laboratory-scale Bridgman furnace (LMC, liquid metal cooling technique) equipped with a  $Y_2O_3/Al_2O_3$  crucible or a conventional  $Al_2O_3$  crucible. Before heating the furnace chamber was vacuumed down to  $5 \times 10^{-3}$  Pa and further backfilled with high purity argon up to 0.05 MPa ( $O_2 < 2$  ppm,  $N_2 < 5$  ppm,  $H_2 < 1$  ppm,  $H_2O < 1$  ppm, and  $CH_4 < 1$  ppm), so as to minimize the oxygen contamination and avoid the evaporation losses of the alloy compositions. Heating temperatures ( $T$ ) were 1550, 1650 and 1750°C, respectively, monitored by a WRe5–WRe26 thermocouple. After 20 min at each of these temperatures, the samples were withdrawn at a constant rate of  $1 \times 10^{-4}$  m·s $^{-1}$ , and quenched into a molten Ga-In-Sn bath upon reaching the withdrawal distance of 120 mm. After DS, some ingots obtained at 1550°C using  $Y_2O_3/Al_2O_3$  crucibles were homogenizing treated. One condition was 950°C for 12 h (HT1). The other was 1100°C for 12 h and then aging at 800°C for 20 h (HT2).

The samples were analyzed by X-ray diffraction (XRD, D/max 2200PC) with Cu K $\alpha$  radiation and electron probe microanalysis (EPMA, JEOL JXA-8100) equipped with energy dispersive X-ray spectroscopy (EDS). The overall oxygen content was measured by the inert gas infrared-thermal conductivity technology (IGI, LECO TC-436). The tensile tests were carried out using an INSTRON-5565

testing machine at room temperature and the loading rate was 0.5 mm/min. The microfracture morphology was observed by scanning electronic microscope (SEM, QUANTA600).

## 3 Results

Figure 1 shows the XRD diffraction patterns of the as-cast and DS alloys obtained at 1550°C. It can be found that the as-cast alloys were consisted of NiTi matrix with a low volume content of  $\beta$ -Nb and  $Ti_2Ni$  phases. In the DS ingot using  $Al_2O_3$  crucibles, TiO and  $(Ti,Al)_4Ni_3O$  phases were detected in addition to NiTi matrix. It reveals that NiTiAl alloys reacted with  $Al_2O_3$  crucibles during the DS, forming a certain amount of oxide inclusions inside the alloys. While in the case of using  $Y_2O_3/Al_2O_3$  crucibles, the phase type was as same as that in the as-cast alloys. No oxide derivatives were emerged in the corresponding XRD patterns.

The typical microstructure of the as-cast and the DS alloys obtained at 1550°C using  $Y_2O_3/Al_2O_3$  crucibles is shown in Figure 2. In the as-cast alloys, the NiTi matrix phase (dark grey and light grey contrast phase) was near equiaxial cellular. Small amounts of  $\beta$ -Nb (white contrast phase) and  $Ti_2Ni$  (black contrast phase) phases intergrew on the grain boundaries (Figure 2a). After DS, the microstructure of cellular-dendrite with short and thick secondary dendrite arm was clearly observed. The cellular crystal trunk and second branch at the side was dark grey NiTi matrix phase. The interdendritic phase was light grey NiTi matrix phase. The  $\beta$ -Nb and  $Ti_2Ni$  phases randomly distributed between the dendritic crystals. Since the Al and

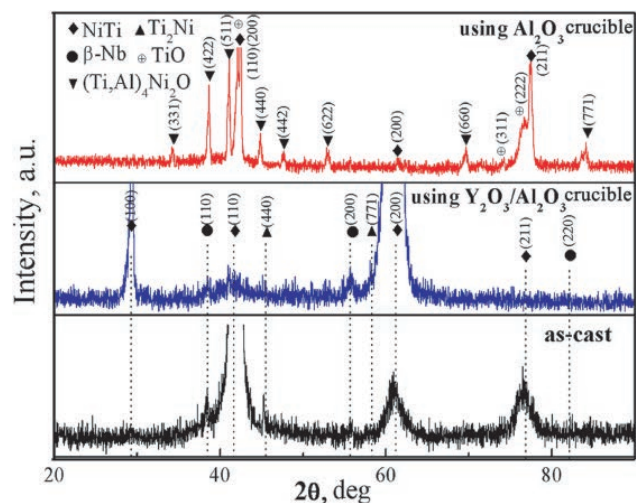
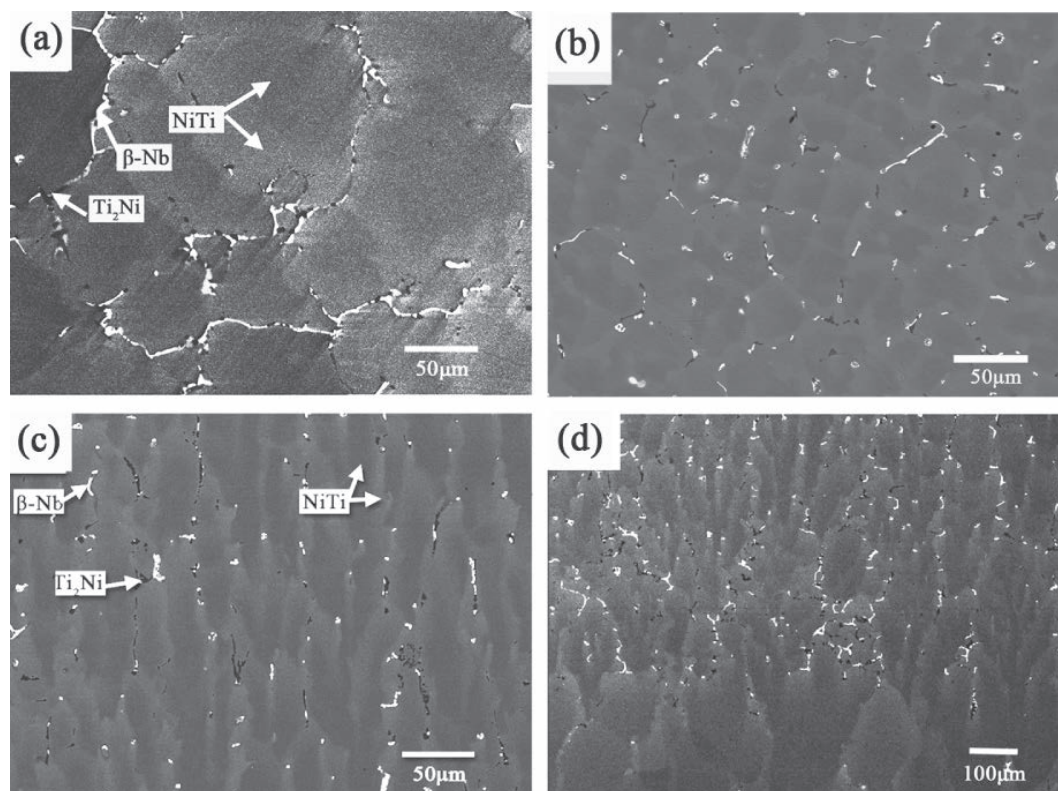


Fig. 1: XRD diffraction patterns of the alloys.



**Fig. 2:** EPMA micrographs of the as-cast and the DS alloys obtained at 1550°C using  $Y_2O_3/Al_2O_3$  crucibles: (a) as-cast; (b) transverse section of the DS steady-state region; (c) longitudinal section of the DS steady-state region; (d) DS initial transition region.

Nb atoms tended to replace the position of Ti atoms in NiTiAl-based alloys [13], based on the microstructure and phase diagram [14] analysis, it is evident that the solidification path of the DS alloys was as follows:  $L \rightarrow NiTi + L \rightarrow NiTi + \beta-Nb + L \rightarrow NiTi + \beta-Nb + Ti_2Ni$ . And the solidified structure preferentially grew along [001] orientation which paralleled to the drawing direction. It was agree with the XRD results that the NiTi matrix phase in the DS alloys was preferred to grow along  $\langle 100 \rangle$  orientation (Figure 1). Therefore, compared with the as-cast alloys, the directional microstructure was effectively produced by DS technique.

In addition, compared with the as-cast alloys, the microstructure of the DS alloys became much finer, and the  $\beta-Nb$  and  $Ti_2Ni$  phases were more dispersed and homogeneous, as shown in the transverse sectional microstructure (Figures 2a and b). The refinement effect was also supported by the interface morphology of the initial transition region (Figure 2d).

Figure 3 presents typical metal-crucible interfacial microstructures when using  $Y_2O_3/Al_2O_3$  crucibles. The metal- $Y_2O_3$  ceramic interface was quite clear and no reaction layer was found. However, in the case of using  $Al_2O_3$  crucibles, a 20  $\mu m$  thick dark  $TiO$  reaction layer at the metal-ceramic interface was observed under the same

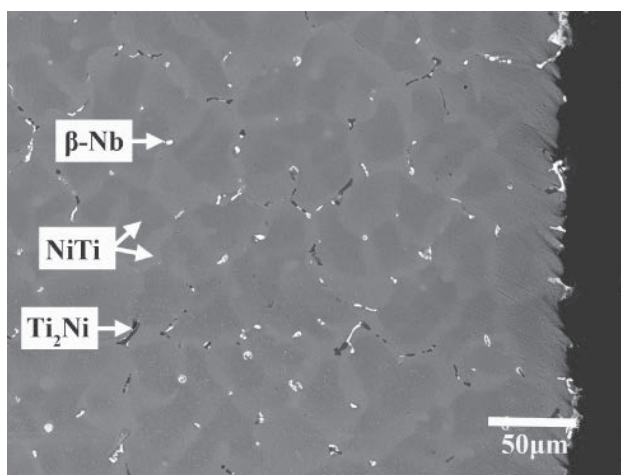


**Fig. 3:** Metal-crucible interfacial microstructure of the ingot in the case of using  $Y_2O_3/Al_2O_3$  crucible at 1550°C.

DS parameter, as shown in Figure 4. Some  $TiO$  and  $(Ti,Al)_4Ni_2O$  phases were also emerged in the alloy matrix (Figures 1 and 4), indicating severe interactions between the molten alloys and the  $Al_2O_3$  during the DS process.

To evaluate the effect of crucible materials on the purification of the alloys, overall oxygen increases in the



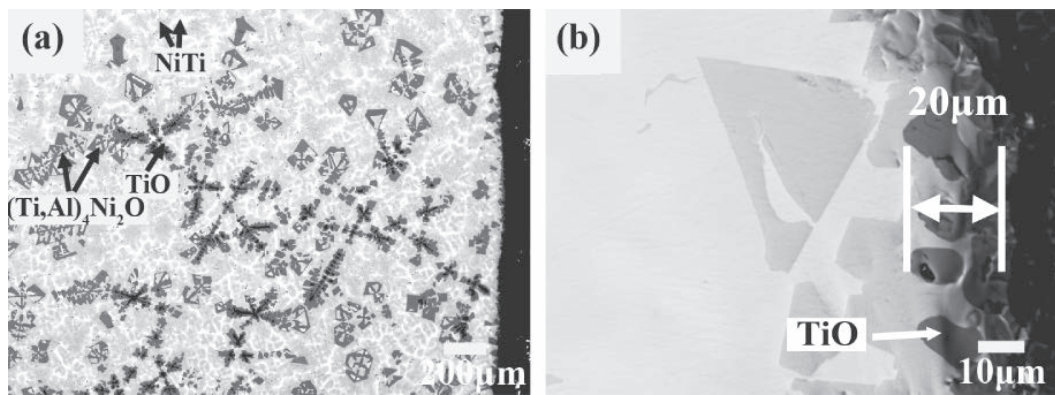


**Fig. 4:** Metal-crucible interfacial microstructures of the ingot in the case of using  $\text{Al}_2\text{O}_3$  crucible at  $1550^\circ\text{C}$  (a) and its higher magnification image (b).

ingots directionally solidified in two different types of crucibles were measured. As shown in Figure 5, the oxygen increase in the DS ingots prepared in an  $\text{Al}_2\text{O}_3$  crucible jumped to 1.006% at  $1550^\circ\text{C}$ , and further increased evidently to 1.336% and 1.366% upon increasing the temperature to  $1650^\circ\text{C}$  and  $1750^\circ\text{C}$ , respectively. However, the oxygen increase of the ingots using  $\text{Y}_2\text{O}_3/\text{Al}_2\text{O}_3$  crucibles was extremely low. At the highest temperature ( $1750^\circ\text{C}$ ), the oxygen increase in the steady-state was only 0.014%. Due to the quenched region above the solid/liquid interface as an enrichment region of the solute, it accumulated a large sum of oxygen due to the floating effect of lighter intercellular liquid with oxygen during the DS process. Thus, the quenched region contained maximum oxygen content. It indicates that even the maximum oxygen increase in the ingot was no more than 0.009% at  $1550^\circ\text{C}$ , 0.032% at  $1650^\circ\text{C}$  and 0.046% at  $1750^\circ\text{C}$ , respectively, as

low as 1/30~1/110 of that using  $\text{Al}_2\text{O}_3$  crucibles. This result revealed very low oxygen contamination referred so far for DS highly reactive alloys in ceramic crucibles [8, 9, 15]. Thus, use of an  $\text{Y}_2\text{O}_3/\text{Al}_2\text{O}_3$  crucible could result in a significant reduction in the oxygen incorporation into the DS alloy matrix.

Tensile testing was carried out to assess the mechanical strength of the alloys before and after DS. The ingots obtained using  $\text{Al}_2\text{O}_3$  crucibles were so brittle that they actually fractured during samples preparation, indicating weak properties. However, for the DS alloys using  $\text{Y}_2\text{O}_3/\text{Al}_2\text{O}_3$  crucibles, the average tensile strength and strain were determined to be 1240 MPa and 2.1%, respectively, which were 91.4% and 75% higher than that of the as-cast alloys (648 MPa and 1.2%), as shown in Figure 6. Its strength increased up to 1328 MPa and 1419 MPa after homogenizing treating in the case of HT1 and HT2, respec-

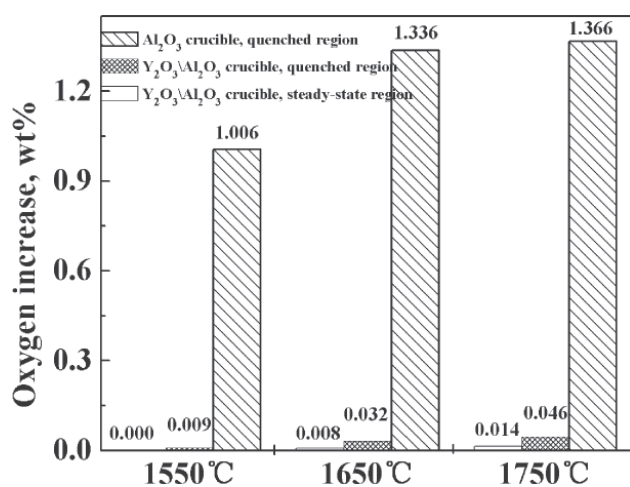


**Fig. 5:** Oxygen increase of the steady-state and quenched regions in the DS ingots using different crucibles.

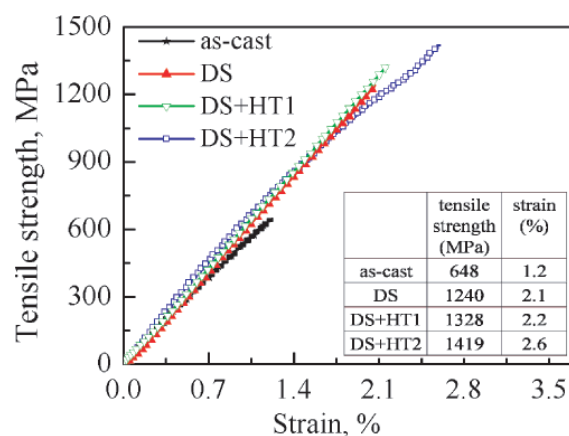


**Fig. 6:** Stress-strain curves for as-cast, DS alloys and DS alloys after homogenizing treatment.

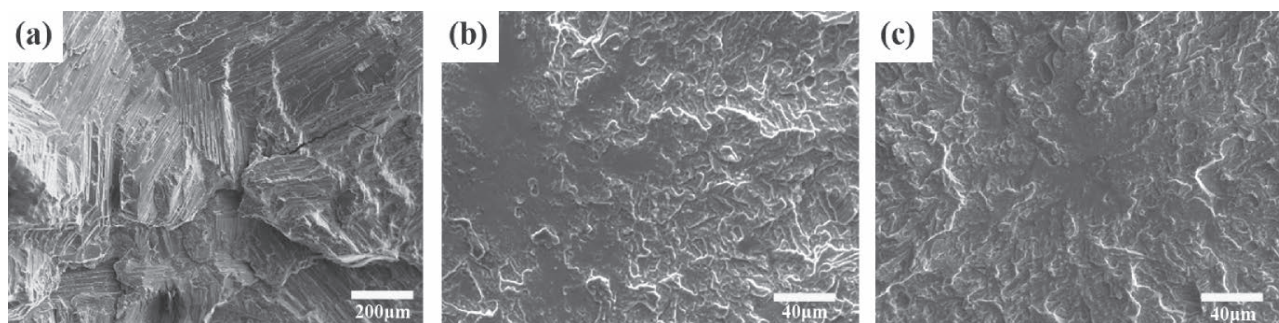


Fig. 7: SEM micrographs of the fracture surfaces: (a) as-cast; (b) DS; (c) DS+HT1.

tively. Such tensile strength exceeded that of the common intermetallic structural materials and superalloy [16].

Melting and casting in ceramic crucibles usually lead to oxygen pickup or/and oxide inclusions in the alloy ingots [17, 18]. As reported by Wang [19], the fracture surfaces of the TiAl alloys contained some  $Y_2O_3$  particles when the alloys were melted in  $Y_2O_3$  crucibles. Due to the deformation incompatibility between the oxide inclusions and the alloy matrix, microcracks easily form in their interfaces, resulting in affecting the tensile strength. However, there were no ceramic inclusions and microcrack found in the DS samples this work, as shown in Figure 7, in agree with no interaction products presence in the alloy matrix (Figures 1, 2 and 3). In addition, compared with the rough fracture surface of the as-cast alloys (Figure 7a), the fracture surface of the DS samples were flat and featureless (Figures 7b and c). Also, it is clear that the microstructure of the DS alloys became finer after DS.

According to the above results, it is obvious that the mechanical properties of the NiTiAl-based alloys had been remarkably improved by the DS technique in novel  $Y_2O_3/Al_2O_3$  ceramic crucibles. One main factor to the improvement is that the microstructure of the alloys was remarkably optimized by the DS technique (Figures 1 and 2). As shown in Figure 2, after DS, effective directional microstructure was formed compared with the as-cast alloy. As the tensile direction was in the same direction as the unidirectional solidified samples, higher values of strength were obtained [20]. Furthermore, it is reported that refinement in microstructure, solid-solution and second-phase constituents in alloys generally contributed to the strength [20]. Therefore, the finer and more homogeneous distribution of  $Ti_2Ni$ ,  $\beta-Nb$  precipitated particles as well as the cellular-dendrite crystals in DS alloys should be helpful to the strength.

Another crucial factor for the tensile improvement is that DS NiTiAl-based alloys using  $Y_2O_3/Al_2O_3$  crucibles assured significant purification effect of the alloys (Figure

5). For highly reactive NiTiAl-based alloys, it is sensitive to the impurity elements (such as oxygen and carbon) and prone to react with crucible materials during the casting process, resulting in the oxygen contamination [21]. Oxygen can not only dissolve in  $Ti_2Ni$  lattice leading to the formation of  $Ti_4Ni_2O_x$  phase, but also promote the direct nucleation of  $Ti_2Ni$  phase [22]. Moreover, other oxide inclusions such as  $TiO$  might be formed. Therefore, high oxygen content during the DS process might alter the desired alloys chemical composition and solidification path by changing the primary solidification phase, consequently influencing the microstructure control and deteriorating the mechanical properties of the alloys. In this work, no chemical reactions between the alloys and  $Y_2O_3$  occurred during the DS process (Figures 1, 2 and 3). The clean ingots contributed to the microstructure control of the alloys. Compared with the severe metal- $Al_2O_3$  crucible reactions (Figures 1 and 4), it is indicated that the  $Y_2O_3$  layer exhibits excellent thermodynamic stability and effective barrier capability to avoid chemical reactions between the  $Al_2O_3$  and the NiTiAl-based alloys. Thus, the combination of low oxygen contamination in the alloys, excellent chemical inertness, high thermal shock resistance and relatively low cost makes the  $Y_2O_3/Al_2O_3$  crucibles very promising candidate crucibles for the DS of highly reactive NiTiAl-based alloys, while the conventional  $Al_2O_3$  crucibles were not suitable due to low thermodynamic stability.

## 4 Conclusions

1. The liquid-metal-cooled directional solidification technique was successfully used to prepare highly reactive NiTiAl-based alloys.
2. Compared with the as-cast alloys fabricated by vacuum arc melting, the microstructure of the DS alloys was effectively optimized and the mechanical

properties remarkably improved when the DS process were performed using novel  $Y_2O_3/Al_2O_3$  crucibles.

3. The tensile strength and strain of the directionally solidified alloys at 1550°C were promoted to 1240 MPa and 2.1% respectively, which were 91.4% and 75% higher than that of the as-cast alloys. The strength increased up to 1328 MPa and 1419 MPa after homogenizing treating.
4. The  $Y_2O_3/Al_2O_3$  crucibles assured significant purification effect of the alloys due to no metal-crucible reactions occurrence. The oxygen increase in the steady-state region of the ingots was no more than 0.014 wt.% even at 1750°C.

**Acknowledgement:** The authors are pleasure to acknowledge the financial support of this research from Natural Science Foundation of China (NSFC) with NSFC grant number of 51101003.

Received: September 26, 2012. Accepted: November 9, 2012.

## References

- [1] Y. Kabiri, A. Kermanpur, A. Foroozmehr, *Vacuum*, 86 (2012), 1073–1077.
- [2] M.H. Elahinia, M. Hashemi, M. Tabesh, S.B. Bhaduri, *Prog. Mater. Sci.*, 57 (2012), 911–946.
- [3] Y. Koizumi, Y. Ro, S. Nakazawa, H. Harada, *Mater. Sci. Eng. A*, 223 (1997), 36–41.
- [4] J. Jung, G. Ghosh, G.B. Olson, *Acta. Mater.*, 51 (2003), 6341–6357.
- [5] H.B. Xu, L.J. Meng, J. Xu, Y. Li, X.Q. Zhao, *Intermetallics*, 15 (2007), 778–782.
- [6] Q. Pan, Master thesis, Beihang University, 2010.
- [7] D.C. Jiang, Y. Tan, S. Shi, W. Dong, Z. Gu, X.L. Guo, *Vacuum*, 86 (2012), 1417–1422.
- [8] U. Hecht, V. Witusiewicz, A. Drevermann, J. Zollinger, *Intermetallics*, 16 (2008), 969–978.
- [9] L.M. Ma, X.X. Tang, B. Wang, L.N. Jia, S.N. Yuan, H. Zhang, *Scripta Mater.*, 67 (2012), 233–236.
- [10] J.H. Perepezko, *Science*, 326 (2009), 1068–1069.
- [11] A. Kostov, B. Friedrich, *Comp. Mater. Sci.*, 38 (2006), 374–385.
- [12] X.X. Tang, H.R. Zhang, M. Gao, H. Zhang, *Chin. Pat.*, (2009), 200910079975.7.
- [13] G. Bozzolo, R.D. Noebe, H.O. Mosca, *J. Alloys Comp.*, 389 (2005), 80–94.
- [14] K. Otsuka, X.B. Ren, *Intermetallics*, 7 (1999), 512–515.
- [15] J. Lapin, Z. Gabalcova, T. Pelachova, *Intermetallics*, 19 (2011), 396–403.
- [16] Y.G. Zhang, Y.F. Han, G.L. Chen, *Structural Intermetallics*, 1st edition, Defense Industry Press, China, 2001.
- [17] R.J. Cui, X.X. Tang, M. Gao, H. Zhang, S.K. Gong, *Mater. Sci. Eng. A*, 541 (2012), 14–21.
- [18] M. Gao, R.J. Cui, L.M. Ma, H.R. Zhang, X.X. Tang, H. Zhang, *J. Mater. Process Technol.*, 211 (2011), 2004–2011.
- [19] L.G. Wang, L.J. Zheng, R.J. Cui, L.L. Yang, H. Zhang, *China Foundry*, 9 (2012), 47–52.
- [20] H. Drar, I.L. Svensson, *Mater. Lett.*, 61 (2007), 392–396.
- [21] Z.H. Zhang, J. Frenzel, K. Neuking, G. Eggeler, *Acta. Mater.*, 53 (2005), 3971–3985.
- [22] L. Zhou, L.J. Zheng, H.R. Zhang, H. Zhang, *Mater. Res. Innov.*, 16 (2012), 115–120.